Distributionally Robust Co-Optimization of Power Dispatch and Do-Not-Exceed Limits

Hongyan Ma, Ruiwei Jiang, *Member, IEEE,* and Zheng Yan

***Abstract*—To address the challenge of the renewable energy uncertainty, the ISO New England (ISO-NE) has proposed to apply do-not-exceed (DNE) limits, which represent the maximum nodal injection of renewable energy the grid can accommodate. Unfortunately, it appears challenging to compute DNE limits that simultaneously maintain the system flexibility and incorporate a large portion of the available renewable energy at the minimum cost. In addition, it is often challenging to accurately estimate the joint probability distribution of the renewable energy. In this paper, we propose a two-stage distributionally robust optimization model that co-optimizes the power dispatch and the DNE limits, by adopting an affinely adjustable power re-dispatch and an adjustable joint chance constraint that measures the renewable utilization. Notably, this model admits a second-order conic reformulation that can be efficiently solved by the commercial solvers (e.g., MOSEK). We conduct case studies based on modified IEEE test instances to demonstrate the effectiveness of the proposed approach and analyze the trade-off among the system flexibility, the renewable utilization, and the dispatch cost.**

***Index Terms*—Power dispatch, renewable energy uncertainty, robust optimization, do-not-exceed limit, affine policy.**

NOMENCLATURE

Indices and Sets

- t, i, k, n, l Index for time period, thermal unit, renewable resource, node, and transmission line, respectively.
- T, I, K, N, L Numbers of time periods, thermal units, renewable resources, nodes, and transmission lines, respectively.
- $[i(n)], [k(n)]$ Sets of thermal units and renewable resources at node n, respectively.
- $[M]$ $[M] := \{1, \ldots, M\}$ for positive integer M.

Parameters

- $C_i(\cdot)$ Fuel cost function of thermal unit i.
- c^+_{kt}, c^-_{kt} Unit cost of overestimating and underestimating the output of renewable resource k during time period t, respectively.
- $\hat{w}_{kt}$ Forecasted output of renewable resource k during time period t.
- d_{nt} Load of node n during time period t.
- $\bar{F}_l$ Transmission capacity limit of line l.
- f_{nl} Shift distribution factor of node n to line l.
- $p_i^{\min}, p_i^{\max}$ Minimum and Maximum generation capacity of thermal unit i, respectively.
- $r_i^{\text{up}}, r_i^{\text{dn}}$ Upward and downward ramp-rate of thermal unit i (MW/min), respectively.
- $\Delta_{\text{d}}, \Delta_{\text{r}}$ Dispatch interval (min) and response time window (min), respectively.
- $w_k^{\min}, w_k^{\max}$ Minimum and maximum generation capacity of renewable resource k, respectively.
- μ_{kt}, σ_{kt} Empirical mean and empirical variance of the prediction error of renewable output k during time period t, respectively.
- δ Weight coefficient between power dispatch and renewable utilization.
- ε_{kt} Random variable representing the output deviation of renewable resource k from its forecast value $\hat{w}_{kt}$ during time period t.
- u_0 Lower bound on renewable utilization.

Decision Variables

- $\hat{p}_{it}$ Scheduled generation amount of thermal unit i during time period t.
- p_{it} Actual generation amount of thermal unit i at time t.
- $\varepsilon^{\text{L}}_{kt}, \varepsilon^{\text{U}}_{kt}$ Lower and upper do-not-exceed limits of ε_{kt}, respectively.
- u Renewable utilization probability.
- B_{ikt}, b_{ikt} Coefficients of the affine decision rule.
- r_{kt}, s_{kt}, z_{kt} Auxiliary dual variables in the reformulation of the adjustable joint chance constraint.

H. Ma and Z. Yan are with the Key Laboratory of Control of Power Transmission and Conversion, Ministry of Education, Department of Electrical Engineering, Shanghai Jiao Tong University, Shanghai 200240, China (e-mail: hahaha91644@sjtu.edu.cn).

R. Jiang is with the Department of Industrial and Operations Engineering, University of Michigan, Ann Arbor, MI 48109, USA (e-mail: ruiwei@umich.edu).

This work is supported in part by the U.S. National Science Foundation (ECCS-1845980) and the National Key R&D Program of China (Technology and application of wind power/photovoltaic power prediction for promoting renewable energy consumption, 2018YFB0904200).

I. INTRODUCTION

THE renewable energy (e.g., wind and solar power) leads to random nodal injections in the power grid and presents a significant challenge to the power system operation. Many methods have been proposed to hedge against the renewable energy uncertainty, including stochastic programming (see, e.g., [1]–[3]) and robust optimization approaches (see, e.g., [4], [5]). These approaches incorporate the uncertainty based on pre-specified models, e.g., probability distribution in stochastic programming (SP) approaches and uncertainty set in robust optimization (RO) approaches. Although SP and RO approaches are widely applied, we may still need to address the following two challenges:

Challenge 1 It may be too costly or even infeasible to treat the renewable energy as non-dispatchable resource

and balance its variation by regulating other dispatchable resources, especially when the renewable penetration is high [6]–[8].

Challenge 2 It is often challenging to accurately estimate the joint probability distribution of the renewable energy. Consequently, the solution obtained from a SP model can perform worse in out-of-sample tests than in the in-sample tests (see, e.g., [9]–[11]).

To address Challenge 1, the ISO-NE proposes an inspiring concept of do-not-exceed (DNE) limits under a given power dispatch strategy [6]. The DNE limits assign an admissible range of renewable energy to each node of the transmission system. This provides a clear guideline for utilizing renewable energy: the system accommodates any nodal injection that lies within the admissible range, and otherwise emergency regulations (e.g., renewable energy curtailment, fast-starting units, and load shedding) may have to be used. In addition, the DNE limits also offer a convenient way of defining and measuring of the system flexibility [12].

Recently, the DNE limits have received increasing attention in the literature. [7], [13] show that the admissible range of a power grid is mathematically equivalent to a polytope. This generalizes the concept of the DNE limits, which take the form of a hypercube. In [6], [7], [13], the admissible range is obtained based on a given power dispatch strategy, which, however, may not be optimal for accommodating renewable generation. As a result, this might underestimate the dispatch capability of the power system in accommodating renewable energy. As an alternative, many studies propose to co-optimize the power dispatch and the DNE limits. [14] proposes a single-stage RO model that co-optimizes the power dispatch and the polytopic admissible range. To incorporate recourse actions (e.g., power re-dispatch), [15] proposes an adjustable RO model in which recourse actions follow an affine decision rule (ADR) with given coefficients. [16] studies an adjustable RO model with ADR and optimized coefficients. Additionally, the proposed model in [16] incorporates risk criteria based on the radius and the coverage probability of the admissible range. Without applying an ADR, [17] considers an adjustable RO model that co-optimizes power dispatch and DNE limits with full recourse. Later, [8] extends [17] by incorporating unit commitment (UC) into the co-optimization, and employs the column-and-constraint generation (CCG) algorithm [18] to solve the proposed model. [19] also considers an adjustable RO model with full recourse that incorporates UC and a polytopic admissible range. Furthermore, [20] considers the risk of the renewable energy being realized outside of the admissible region, which result in, e.g., curtailment of renewable energy. Differently, [21] models this risk by maximizing the probability that the renewable energy being realized within the DNE limits. Then, this model is solved by using the sample average approximation algorithm. [22] considers an adjustable RO model with both discrete and continuous recourse and proposes to solve this model with a nested CCG algorithm. [23] incorporates topology control into the co-optimization and considers zonal DNE limits. Similarly, [24] also considers topology control and proposes a multistage framework to improve the computational efficacy. It is worth mentioning that solving the adjustable RO model with full recourse requires repeatedly solving mixed-integer programs with big-M coefficients (see, e.g., [8], [13], [20], [23]), which may be challenging when many nodes of the power grid incorporate renewable energy.

A natural way of mitigating Challenge 2 is to employ distributionally robust optimization (DRO). In contrast to SP that considers a single probability distribution, DRO considers a family of probability distributions that are plausible of modeling the renewable energy. We term the family of distributions as an ambiguity set. In the existing literature, ambiguity sets based on the moments of uncertainty (e.g., mean, variance, etc.) are commonly applied (see, e.g., [25]–[28]). Other distributional information based on, e.g., the Wasserstein distance [29], [30], the ϕ-divergence [11], [31], and the unimodality [16], [32], [33], have also been proposed to characterize the ambiguity set. Accordingly, DRO formulates a robust counterpart of SP and hedges against the worst-case probability distribution within the ambiguity set.

In this paper, we consider a distributionally robust (DR) co-optimization model for the power dispatch and the DNE limits. Our model follows [20], [21] to incorporate the operational risks. The main contributions of this paper are summarized as follows.

1) We propose and incorporate adjustable DR joint chance constraints into the DNE model. This incorporation improves the out-of-sample performance on renewable utilization and dispatch cost, and provides a clear picture of the trade-off between these two performance metrics.
2) The optimization of the DNE limits results in a (computationally prohibitive) two-stage RO formulation with a decision-dependent uncertainty set. By using ADR with optimized coefficients, we show that this problem admits a conservative approximation based on linear constraints, which can be efficiently handled in commercial solvers. This improves the scalability of the DNE approach.
3) In an extensive case study, we demonstrate the improved out-of-sample performance and scalability of the proposed approach based on various systems, including the IEEE 14-, 118-, and 300-bus systems.

This paper focuses on the renewable generation uncertainty, but the proposed approach can be extended to handle other uncertainties (such as load uncertainty and contingencies) with slight changes. In addition, the proposed model assumes a fixed UC and power grid topology. Nevertheless, these decisions can also be incorporated into this model with slight changes, leading to mixed 0-1 conic programming reformulations.

The remainder of this paper is organized as follows. Section II presents the mathematical formulation and Section III describes the solution methodology. Section IV extends the model and solution methodology to incorporate alternative operational risks. Section V reports the case studies that demonstrate the effectiveness of the proposed approach, before we draw conclusions in Section VI.

II. Mathematical Formulation

We describe the co-optimization model of power dispatch and DNE limits in Section II-A and the adjustable DR chance constraint in Sections II-B.

A. DNE Limits

Given the forecasted renewable energy outputs $\hat{w}_{kt}$, the nominal economic dispatch (ED) model maintains the generation-load balance under operational restrictions. Mathematically, we formulate the constraints of a multi-period nominal ED model as follows:

$$\sum_{i\in[I]} \hat{p}_{it} + \sum_{k\in[K]} \hat{w}_{kt} = \sum_{n\in[N]} d_{nt},\ \forall t\in[T], \tag{1a}$$

$$-\bar{F}_l \le \sum_{n\in[N]} f_{nl}\left(\sum_{i\in[i(n)]} \hat{p}_{it} + \sum_{k\in[k(n)]} \hat{w}_{kt} - d_{nt}\right) \le \bar{F}_l,$$
$$\forall l\in[L],\ \forall t\in[T], \tag{1b}$$

$$p_i^{\min} \le \hat{p}_{it} \le p_i^{\max},\ \forall i\in[I],\ \forall t\in[T], \tag{1c}$$

$$-r_i^{\mathrm{dn}}\Delta_{\mathrm{d}} \le \hat{p}_{it} - \hat{p}_{i,t-1} \le r_i^{\mathrm{up}}\Delta_{\mathrm{d}},\ \forall i\in[I],\ \forall t\in[T], \tag{1d}$$

where $\hat{p}_{it}$ represents the pre-dispatch strategy based on the forecast renewable generation $\hat{w}_{kt}$, constraints (1a) represent the generation-load balance, (1b) represent the transmission line capacity restrictions based on the dc approximation of the power flow equations, (1c) represent the capacity limits of the thermal units, and (1d) represent the ramp-rate limits of the thermal units. When taking the uncertainty of renewable energy and the DNE limits into account, the power system aims to accommodate any nodal injections of renewable energy through corrective power re-dispatch, as long as such injections lie within the DNE limits. We formulate this requirement as follows for all $t\in[T]$:

$$\forall \varepsilon_t\in[\varepsilon_t^{\mathrm{L}},\varepsilon_t^{\mathrm{U}}],\ \text{there exist } \{p_{it}(\varepsilon_t)\}_{i\in[I]} \text{ such that:}$$

$$\sum_{i\in[I]} p_{it}(\varepsilon_t) + \sum_{k\in[K]} (\hat{w}_{kt}+\varepsilon_{kt}) = \sum_{n\in[N]} d_{nt}, \tag{2a}$$

$$-\bar{F}_l \le \sum_{n\in[N]} f_{nl}\left(\sum_{i\in[i(n)]} p_{it}(\varepsilon_t) + \sum_{k\in[k(n)]} (\hat{w}_{kt}+\varepsilon_{kt})\right)$$
$$-\sum_{n\in[N]} f_{nl}d_{nt} \le \bar{F}_l,\ \forall l\in[L], \tag{2b}$$

$$p_i^{\min} \le p_{it}(\varepsilon_t) \le p_i^{\max},\ \forall i\in[I], \tag{2c}$$

$$-r_i^{\mathrm{dn}}\Delta_{\mathrm{d}} \le p_{it}(\varepsilon_t) - p_{i,t-1}(\varepsilon_{t-1}) \le r_i^{\mathrm{up}}\Delta_{\mathrm{d}},\ \forall i\in[I], \tag{2d}$$

$$-r_i^{\mathrm{dn}}\Delta_{\mathrm{r}} \le p_{it}(\varepsilon_t) - \hat{p}_{it} \le r_i^{\mathrm{up}}\Delta_{\mathrm{r}},\ \forall i\in[I], \tag{2e}$$

where constraints (2a)–(2d) are counterparts of (1a)–(1d) with regard to the power re-dispatch variables $p_{it}(\varepsilon_t)$ and constraints (2e) represent the ramping capacity limits within the response time window. In this paper, we assume that $p_{it}(\varepsilon_t)$ follows an ADR, i.e., $p_{it}(\varepsilon_t)$ is the following affine function of ε_t:

$$p_{it}(\varepsilon_t) = \hat{p}_{it} + \sum_k (B_{ikt}\varepsilon_{kt} + b_{ikt}),\ \forall i\in[I],\ \forall t\in[T], \tag{2f}$$

where B_{ikt} and b_{ikt} represent the response of $p_{it}(\varepsilon_t)$ to the forecast error ε_t and can be adjusted to optimize the objective function (to be specified in Section II-B). On the one hand, the ADR corresponds to the incremental output of the automatic generation control (AGC) units as an affine function of the renewable generation deviation. For the non-AGC units, we can set $B_{ikt} = b_{ikt} = 0$. On the other hand, the ADR restricts the search space of the recourse variables $p_{it}(\varepsilon_t)$ and so yields a conservative approximation of the constraints (2a)–(2e).

B. Adjustable DR Joint Chance Constraints

We note that formulations (1a)–(1d) and (2a)–(2e) do not incorporate any distributional information of the forecast error ε_{kt}. This may cause a mismatch between the DNE limits and renewable energy. For example, it may be unlikely that the renewable generation is realized within the DNE limits, and accordingly we may curtail a significant portion of the renewable generation. To address this challenge, we first designate that the DNE limits contain the forecasted output of renewable energy and lie within the capacity limits of the renewable generation:

$$w_k^{\min} \le \hat{w}_{kt} + \varepsilon_{kt}^{\mathrm{L}} \le \hat{w}_{kt} + \varepsilon_{kt}^{\mathrm{U}} \le w_k^{\max},$$
$$\forall k\in[K],\ \forall t\in[T]. \tag{3}$$

Second, we consider an *adjustable* joint chance constraint to measure the utilization of renewable energy:

$$\inf_{\mathbb{P}\in\mathcal{D}} \mathbb{P}\left(\varepsilon_t\in[\varepsilon_t^{\mathrm{L}},\varepsilon_t^{\mathrm{U}}]\right) \ge u,\ \forall t\in[T], \tag{4a}$$

$$u_0 \le u \le 1, \tag{4b}$$

where u estimates the probability of fully utilizing the renewable energy and u_0 represents a lower bound of u. In this paper, we assume that $u_0 > 2/3$ (see Theorem 1). This assumption is not very restrictive because power system operators often desire high utilization of renewable energy (see, e.g., [34]). Additionally, we note that u represents a decision variable in our model and can be adjusted to optimize the trade-off between the power dispatch cost and the renewable utilization. In addition, we consider an ambiguity set $\mathcal{D}$ consisting of probability distributions $\mathbb{P}$ that (i) match the empirical mean μ_{kt} and empirical variance σ_{kt} of each ε_{kt} and (ii) is unimodal about μ_{kt}, i.e.,

$$\mathcal{D} := \left\{ \mathbb{P}: \begin{array}{l} \mathbb{E}_{\mathbb{P}}[\varepsilon_{kt}] = \mu_{kt},\ \mathrm{Var}(\varepsilon_{kt}) = \sigma_{kt}^2, \\ \varepsilon_{kt} \text{ is unimodal about } \mu_{kt},\ \forall k\in[K], \forall t\in[T] \end{array} \right\}. \tag{5}$$

Unimodality about μ_{kt} indicates that the probability density function of ε_{kt}, if exists, is nondecreasing from 0 to μ_{kt} and is nonincreasing afterwards. In the literature, many probability distributions proposed for modeling the renewable energy forecast error are unimodal (see, e.g., [35]–[37]). It is worth mentioning that [16] consider the unimodality of the *joint* probability distribution $\mathbb{P}$ of all ε_{kt}. In contrast, the unimodality in $\mathcal{D}$ is with respect to the *marginal* distribution of each ε_{kt}, which is weaker than the joint unimodality assumed in [16] and easier to verify by the historical data. In addition, the ambiguity set $\mathcal{D}$ leads to a polynomially solvable reformulation (see Section III).

We close this section by formulating the DR co-optimization (DRCO) model of power dispatch and DNE limits:

$$\min_{\substack{\hat{p},B,b,\\ \varepsilon^{\text{L}},\varepsilon^{\text{U}},u}} \sum_{t\in[T]}\sum_{i\in[I]} C_i(\hat{p}_{it}) - \delta u \tag{6a}$$

$$\text{s.t.} \;\; \text{(1a)–(1d)},\ \text{(2a)–(2f)},\ \text{(3)},\ \text{(4a)–(4b)}, \tag{6b}$$

where the objective function (6a) contains two terms, with the first term representing the power dispatch cost and the second representing the renewable utilization u, which is amplified by a weight δ. The system operator can set δ based on her trade-off between the renewable utilization and the dispatch cost. If δ is close to zero then the dispatch cost and the renewable utilization are low. As δ increases, both dispatch cost and renewable utilization increase. By gradually increasing the value of δ and re-solving model (6a)–(6b), we obtain a cost-utilization frontier that can clearly indicate the trade-off between these two performance measures (see Section V for related case studies).

III. Solution Methodology

We recast the DRCO model (6a)–(6b) as a second-order conic program that is polynomially solvable. For notation brevity, we derive based on abstract notation. First, we represent constraints (2a)–(2f) in the following abstract form:

$$\exists\ \varepsilon^{\text{L}},\varepsilon^{\text{U}},p(\varepsilon):$$
$$Tx + Wp(\varepsilon) \le H\varepsilon,\ \forall \varepsilon\in[\varepsilon^{\text{L}},\varepsilon^{\text{U}}], \tag{7a}$$
$$p(\varepsilon) = B\varepsilon + b, \tag{7b}$$

where $p(\varepsilon)$ denotes the power re-dispatch variables, matrices T, W, and H denote the given parameters in constraints (2a)–(2e), and matrix B and vector b denote the variables in the ADR (2f). Letting $E := \text{diag}(\varepsilon^{\text{U}} - \varepsilon^{\text{L}})$, we represent the hypercube $[\varepsilon^{\text{L}},\varepsilon^{\text{U}}]$ as $\{\varepsilon^{\text{L}} + Ev : v\in[0,e]\}$, where e denotes the vector of all ones. Then, we recast (7a)–(7b) as

$$\exists\ \varepsilon^{\text{L}},\varepsilon^{\text{U}},B,b:$$
$$Tx + W\big(BEv + B\varepsilon^{\text{L}} + b\big) \le H\varepsilon^{\text{L}} + HEv,$$
$$\forall v\in[0,e]. \tag{7c}$$

We claim that (7c) is equivalent to

$$\exists\ \varepsilon^{\text{L}},\varepsilon^{\text{U}},S,s_0:$$
$$Tx + W(Sv + s_0) \le H\varepsilon^{\text{L}} + HEv,\ \forall v\in[0,e]. \tag{7d}$$

We now prove the equivalence (7c) $\Leftrightarrow$ (7d). One the one hand, suppose that there exist B and b such that (7c) holds valid. Then, we let $\bar{S} = BE$ and $\bar{s}_0 = B\varepsilon^{\text{L}} + b$ to yield $Tx + W(\bar{S}v + \bar{s}_0) \le H\varepsilon^{\text{L}} + HEv$ for all $v\in[0,e]$. Hence, (7c) implies (7d). On the other hand, suppose that there exist S and s_0 such that (7d) holds valid. Then, we let $\bar{B} = SE^{-1}$ and $\bar{b}_0 = s_0 - SE^{-1}\varepsilon^{\text{L}}$ to yield $Tx + W(\bar{B}Ev + \bar{B}\varepsilon^{\text{L}} + \bar{b}_0) \le H\varepsilon^{\text{L}} + HEv$ for all $v\in[0,e]$. Hence, (7d) also implies (7c). Furthermore, we note that constraint (7d) holds valid if and only if $\sup_{v\in[0,e]}\{(WS - HE)v\} \le H\varepsilon^{\text{L}} - Tx - Ws_0$, where the supremum operator is applied on each component of $(WS - HE)v$. Using the standard technique in robust optimization (see, e.g., [38]), we recast this constraint, and so constraints (2a)–(2f), as the following linear inequalities:

$$\exists\ \varepsilon^{\text{L}},\varepsilon^{\text{U}},S,s_0,R:$$
$$Re \le H\varepsilon^{\text{L}} - Tx - Ws_0, \tag{7e}$$
$$R \ge WS - HE,\ R\ge 0. \tag{7f}$$

Second, we recast the adjustable DR joint chance constraint (4a) as second-order conic constraints. We present this result in the following theorem and its proof in Appendix A.

Theorem 1: If $u > 2/3$, then, for all $t\in[T]$, chance constraint (4a) is equivalent to the following constraints:

$$\left\|\begin{bmatrix}\sqrt{\frac{8}{3}}\\ r_{kt} - z_{kt}\end{bmatrix}\right\|_2 \le r_{kt} + z_{kt},\ \forall k\in[K], \tag{8a}$$
$$\left\|\begin{bmatrix}s_{kt} - 1\\ 2z_{kt}\end{bmatrix}\right\|_2 \le s_{kt} + 1,\ \forall k\in[K], \tag{8b}$$
$$\sigma_{kt} r_{kt} \le \mu_{kt} - \varepsilon^{\text{L}}_{kt},\ \forall k\in[K], \tag{8c}$$
$$\sigma_{kt} r_{kt} \le \varepsilon^{\text{U}}_{kt} - \mu_{kt},\ \forall k\in[K], \tag{8d}$$
$$\sum_{k\in[K]} s_{kt} \le 1 - u, \tag{8e}$$
$$r_{kt}, s_{kt}, z_{kt} \ge 0,\ \forall k\in[K]. \tag{8f}$$

To summarize, the DRCO model (6a)–(6b) is equivalent to the following second-order conic program:

$$\min_{\substack{\hat{p},S,s_0,R,u,\\ \varepsilon^{\text{L}},\varepsilon^{\text{U}},r,s,z}} \sum_{t\in[T]}\sum_{i\in[I]} C_i(\hat{p}_{it}) - \delta u \tag{9a}$$

$$\text{s.t.} \;\; \text{(1a)–(1d)},\ \text{(7e)–(7f)},\ \text{(3)},\ \text{(4b)},\ \text{(8a)–(8f)}. \tag{9b}$$

It is well-known in the optimization literature that second-order conic programs like (9a)–(9b) can be solved in time polynomial of the problem inputs. Specifically, (9a)–(9b) involves $\mathcal{O}((I+L)KT)$ many linear constraints and $\mathcal{O}(KT)$ many conic constraints, each based on a 3-dimensional second-order cone. Then, by Theorem 5.4 in [46], the primal-dual path-following algorithms using the Nesterov-Todd direction and large-update methods solve (9a)–(9b) to any precision ϵ in $\mathcal{O}(\sqrt{KT}\log(1/\epsilon))$ many iterations and each iteration needs at most $\mathcal{O}((I+L)^3K^3T^3)$ many arithmetic operations.

IV. Extension to Alternative Operational Risks

We extend the DRCO model (6a)–(6b) by considering alternative operational risks of the chance constraint (4a), which computes the expected costs incurred by overestimating/underestimating the renewable energy. We note that such operational risks are studied in [20]. In this paper, we study the DR counterpart of the risks based on the ambiguity set $\mathcal{D}$ defined in (5). Specifically, the DR expected cost of overestimation/underestimation are defined as

$$P^{+}(\varepsilon^{\text{L}},\varepsilon^{\text{U}}) := \sup_{\mathbb{P}\in\mathcal{D}} \mathbb{E}_{\mathbb{P}}\left[\sum_{k\in[K]}\sum_{t\in[T]} c^{+}_{kt}\left[\varepsilon^{\text{L}}_{kt} - \varepsilon_{kt}\right]^{+}\right],$$
$$P^{-}(\varepsilon^{\text{L}},\varepsilon^{\text{U}}) := \sup_{\mathbb{P}\in\mathcal{D}} \mathbb{E}_{\mathbb{P}}\left[\sum_{k\in[K]}\sum_{t\in[T]} c^{-}_{kt}\left[\varepsilon_{kt} - \varepsilon^{\text{U}}_{kt}\right]^{+}\right],$$

where $[x]^+ = \max\{x, 0\}$ for $x \in \mathbb{R}$. When $\varepsilon_{kt} \notin [\varepsilon^{\text{L}}_{kt}, \varepsilon^{\text{U}}_{kt}]$, emergency regulations (e.g., renewable generation curtailment, fast-starting units, and load shedding) may be needed to recover the operational feasibility. Accordingly, the cost coefficients c^+_{kt} and c^-_{kt} should be estimated based on the corresponding regulations (e.g., the opportunity/penalty cost of curtailing renewable generation, the estimated real-time price of using fast-starting units, and the penalty cost of shedding load). Then, the DRCO model (6a)–(6b) can be extended by incorporating $P^{\pm}(\varepsilon^{\text{L}}, \varepsilon^{\text{U}})$as follows:

$$\min_{\substack{\hat{p},B,b,\\ \varepsilon^{\text{L}},\varepsilon^{\text{U}},u}} \sum_{t\in[T]}\sum_{i\in[I]} C_i(\hat{p}_{it}) - \delta u + \delta^+ P^+(\varepsilon^{\text{L}}, \varepsilon^{\text{U}}) + \delta^- P^-(\varepsilon^{\text{L}}, \varepsilon^{\text{U}})$$

$$\text{s.t.} \quad \text{(1a)–(1d)}, \ \text{(2a)–(2f)}, \ \text{(3)}, \ \text{(4a)–(4b)},$$

where δ^+ and δ^- represent the weights on the expected costs of overestimation/underestimation, respectively.

We compute $P^{\pm}(\varepsilon^{\text{L}}, \varepsilon^{\text{U}})$ by solving conic programs. We present this result in the following theorem and its proof in Appendix B. Accordingly, the extended DRCO model presented above can be recast as a conic program that can be efficiently solved by commercial solvers.

Theorem 2: Let $g(\{(c_{kt}, \tau_{kt})\}_{k\in[K],t\in[T]})$ represent the optimal value of the following conic program:

$$\min_{\pi_{\ell kt},\Lambda_{ktij}} \ \sqrt{3}\sum_{k\in[K]}\sum_{t\in[T]} c_{kt}\sigma_{kt}(\pi_{1kt} + \pi_{3kt} + 1) \tag{10a}$$

$$\text{s.t.} \ \Lambda_{kt00} = \tau_{kt}, \ \forall k \in [K], \ \forall t \in [T], \tag{10b}$$

$$\left\| \begin{bmatrix} \pi_{2kt} \\ \pi_{1kt} - \pi_{3kt} + 1 \end{bmatrix} \right\|_2 \le \pi_{1kt} + \pi_{3kt} + 1, \quad \forall k \in [K], \ \forall t \in [T], \tag{10c}$$

$$\sum_{i,j:\ i+j=2\ell-1} \Lambda_{ktij} = 0, \quad \forall \ell = 1,2,3, \ \forall k \in [K], \ \forall t \in [T], \tag{10d}$$

$$\sum_{i,j:\ i+j=2\ell} \Lambda_{ktij} = \pi_{\ell kt}, \quad \forall \ell = 1,2,3, \ \forall k \in [K], \ \forall t \in [T], \tag{10e}$$

$$\Lambda_{kt} \in \mathbb{S}^{4\times 4}_+, \ \forall k \in [K], \ \forall t \in [T], \tag{10f}$$

where $\mathbb{S}^{4\times4}_+$ represents the cone of all 4×4 positive semidefinite matrices. Then, we have

$$P^+(\varepsilon^{\text{L}}, \varepsilon^{\text{U}}) = g\left(\left\{\left(c^+_{kt}, \frac{\mu_{kt} - \varepsilon^{\text{L}}_{kt}}{\sqrt{3}\sigma_{kt}}\right)\right\}_{k\in[K],t\in[T]}\right),$$

$$P^-(\varepsilon^{\text{L}}, \varepsilon^{\text{U}}) = g\left(\left\{\left(c^-_{kt}, \frac{\varepsilon^{\text{U}}_{kt} - \mu_{kt}}{\sqrt{3}\sigma_{kt}}\right)\right\}_{k\in[K],t\in[T]}\right),$$

Furthermore, $P^{\pm}(\varepsilon^{\text{L}}, \varepsilon^{\text{U}})$ can be conservatively approximated by piecewise linear functions of $(\varepsilon^{\text{L}}, \varepsilon^{\text{U}})$ with arbitrary precision.

V. Case Studies

We carry out numerical case studies on modified IEEE 14-bus and IEEE 118-bus systems. All programs are developed using MATLAB2014a and solved by MOSEK via YALMIP 11.5 on a laptop with a 2.7GHz Intel Core i5 CPU and 8GB RAM.

A. The Modified IEEE 14-bus System

In this system, there are 20 transmission lines and 5 generators (G1–G5) providing corrective power re-dispatch. The generators and network characteristics can be found in MATPOWER [39]. Two wind power farms with 80 MW (W1) and 100MW (W2) installed capacity are connected to the system at nodes 5 and 7, respectively. The load profile is from [19] and scaled by a factor of 0.1. We set $\Delta_d = 60$min, $\Delta_r = 5$min, $T = 24$hr, and $p^{\min}_i = 0.1p^{\max}_i$ for all $i \in [I]$.

B. The Cost-Utilization Frontier and the DNE Limits

To demonstrate the trade-off between the dispatch cost and the utilization of renewable energy, we generate a cost-utilization frontier by gradually increasing the value of δ and re-solving the DRCO model (6a)–(6b) for each δ. To this end, we first obtain the wind power forecast of W1 and W2 from the NREL Eastern Wind Dataset [40]. We generate a set of wind power prediction error data by using Gaussian distribution, whose mean is set to be 0 for all $t \in [T]$ and variance increases from 10% of the installed capacity by 0.1% as t increases from 1 to T. Second, we divide the data into two parts. We use the first part to calibrate the ambiguity set $\mathcal{D}$ based on the empirical mean and variance. Then, for fixed δ, we solve the DRCO model to obtain the optimal DNE limits $[\varepsilon^{\text{L}*}, \varepsilon^{\text{U}*}]$ and the minimum power dispatch cost $\sum_{t\in[T]}\sum_{i\in[I]} C_i(\hat{p}^*_{it})$, where $\hat{p}^*$ represents an optimal solution of $\hat{p}$. We use the second part of the data to obtain an out-of-sample empirical estimate of the renewable utilization probability $\mathbb{P}\{\varepsilon \in [\varepsilon^{\text{L}*}, \varepsilon^{\text{U}*}]\}$. Third, we repeat the second step by gradually increasing the value of δ from 1 to 38000. We set the step length as 100 when $\delta \le 1000$, 400 when $\delta \in (1000, 5000]$, 1000 when $\delta \in (5000, 10000]$, and 4000 when $\delta > 10000$. Accordingly, we obtain 33 groups of minimum power dispatch costs, optimal DNE limits, and the corresponding renewable utilization probabilities.

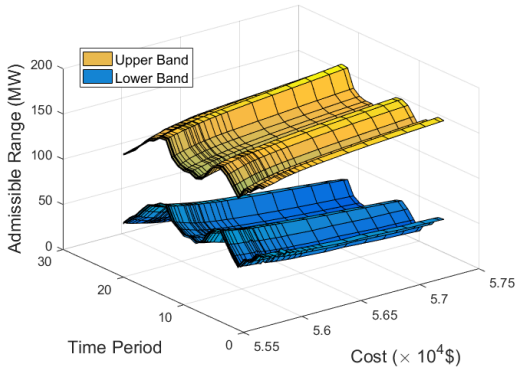

Fig. 1: Minimum Dispatch Costs vs. Admissible Ranges of Wind Power, with $r^{\text{up}}_i = r^{\text{dn}}_i = 2.0\% \times p^{\max}_i$ for all $i \in [I]$

In Fig. 1, we display the minimum power dispatch cost and the optimal DNE limits under various δ values. For intuitive presentation, we shift the DNE limits to obtain the admissible ranges of wind power $[w^{\text{L}}_t, w^{\text{U}}_t] := [\sum_{k\in[K]}(\mu_{kt} + \varepsilon^{\text{L}}_{kt}), \sum_{k\in[K]}(\mu_{kt} + \varepsilon^{\text{U}}_{kt})]$. The interpretation of each pair of

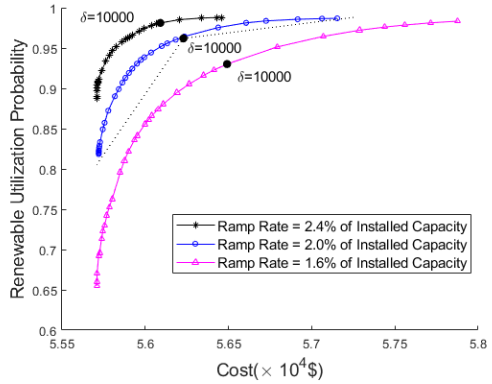

Fig. 2: The Cost-Utilization Frontier under Various Ramping Capabilities

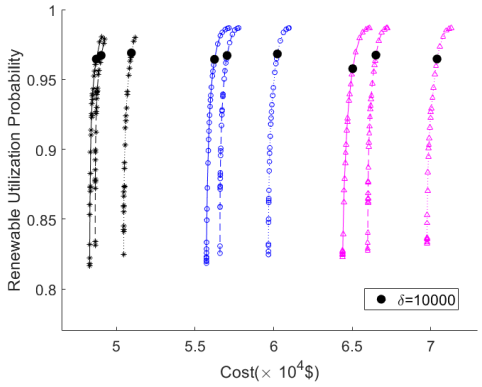

Fig. 3: The Cost-Utilization Frontier under Various System Load Levels and Network Topology. The load levels of the left three, middle three, and right three curves are 0.9, 1.0, and 1.1 multiples of the original load level, respectively. Under each load level, the topology associated with the 3 curves from left to right is original topology, line 7 open, and line 1 capacity reduction, respectively.

points $(t, C_{\text{min}}, w_t^{\text{L}})$ and $(t, C_{\text{min}}, w_t^{\text{U}})$ is that, during time period t, we need to spend at least C_{min} on power dispatch in order to accommodate any total wind power output within the interval $[w_t^{\text{L}}, w_t^{\text{U}}]$. From Fig. 1, we observe that the admissible range of wind power broadens as the minimum dispatch cost increases. This indicates that the power system can become more flexible as we invest more on power dispatch.

To take a closer look at the trade-off between the dispatch cost and the renewable utilization, we display the cost-utilization frontiers under various ramping capabilities in Fig. 2. Specifically, we consider three ramping capabilities in which r_i^{up} and r_i^{dn} equal 1.6%, 2.0%, and 2.4% of $p_i^{\max}$ for all $i \in [I]$, respectively. For each capability and for each δ value, we depict the minimum power dispatch cost versus the smallest renewable utilization probability in all time periods. From Fig. 2, we first observe that the renewable utilization increases as the dispatch cost increases, confirming our observation from Fig. 1. Second, the increasing trend of renewable utilization diminishes as the dispatch cost increases. Take the middle curve with 2% ramping capability for example. On this curve, we highlight two segments with $\delta \leq 10,000$ and $\delta > 10,000$, respectively. The first segment reflects a 19.5% increase in renewable utilization with only an 0.9% increase in the power dispatch cost (i.e., increasing by \$521). This translates into a 0.037%/\$ increasing rate of the renewable utilization. On the contrary, the second segment reflects a 2.7% increase in renewable utilization with a 1.8% increase in the power dispatch cost (i.e., increasing by \$1021). This translates into a 0.003%/\$ increasing rate of the renewable utilization. This observation indicates that a small additional investment on power dispatch can quickly enhance the renewable utilization, but this investment becomes less efficient when the utilization is already high. Third, we observe from Fig. 2 that the frontier rises as the ramping capability increases. For example, to achieve a 95% renewable utilization, it costs 5.67×10^4\$ when the ramping capability is 1.6%, 5.61×10^4\$ when the ramping capability is 2.0%, and 5.58×10^4\$ when the ramping capability is 2.4%. This observation indicates that a small enhancement on the ramping capability can significantly improve the cost-effectiveness of utilizing renewable energy.

In addition, we test the dynamics of the cost-utilization frontier under various system states and report the results in Fig. 3. From this figure, we observe that the cost-utilization frontier remains almost unchanged in shape and only shifts horizontally as the system state changes. In addition, the impact of network topology on this frontier becomes more significant as the system load increases. Furthermore, for a fixed value of δ, the system states have limited impacts on the renewable utilization. For example, when we set δ as 10,000, the dispatch cost significantly changes under different system states, while the renewable utilization remains almost the same (see the nine solid dots in Fig. 3). This indicates that, once the system operator sets δ based on her cost-utilization trade-off, the guaranteed renewable utilization is insensitive to the system states.

C. Comparisons with the Original DNE Limit Approach

We compare the proposed DRCO model (termed the IDNE approach) with the original DNE approach (termed ODNE) in [6], which computes the DNE limits based on a given dispatch strategy without explicitly modeling the renewable ambiguity. Besides, to demonstrate the value of the DR chance constraints (DRCC), we also compare with an intermediate model that incorporates DRCC into the ODNE model (termed ODNE+DRCC). We randomly generate 5,000 out-of-sample scenarios of wind prediction errors from the hypothetical Gaussian distribution and compare (i) the optimal DNE limits, (ii) the renewable utilization probability, and (iii) the actual cost incurred in each scenario. The actual cost consists of the pre-dispatch cost, the corrective re-dispatch cost which is the incremental cost over the pre-dispatch cost, and the penalty costs which are incurred (a) when $\varepsilon_{kt} < \varepsilon_{kt}^{\text{L}}$, the load shedding takes place at a cost of 2,000\$/MW and (b) when $\varepsilon_{kt} > \varepsilon_{kt}^{\text{U}}$, the renewable energy is curtailed at a cost of 100\$/MW. Renewable curtailment incurs a cost due to the loss of opportunity in generating electricity and the loss of

environmental benefit. In all comparisons, we set $\delta = 10,000$ and $r_i^{\text{up}} = r_i^{\text{dn}} = 2.0\% \times p_i^{\max}$ for all $i \in [I]$.

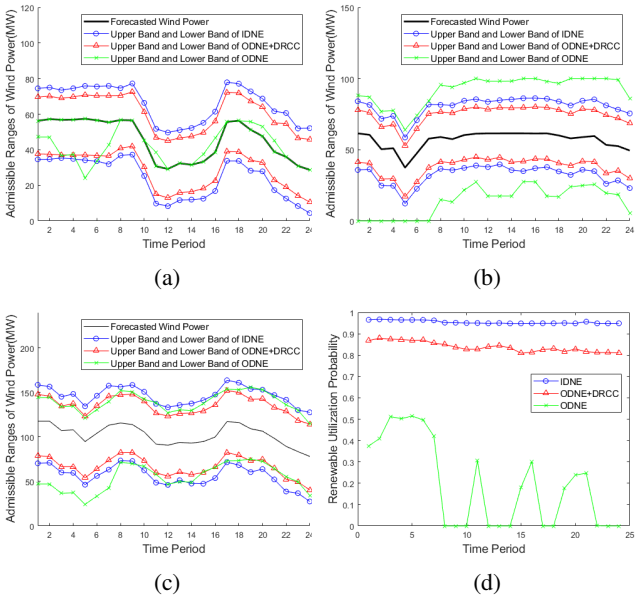

Fig. 4: Comparisons of ODNE, ODNE+DRCC, and IDNE on (a) Admissible Ranges of W1, (b) Admissible Ranges of W2, (c) Total Admissible Ranges of Wind Power, and (d) Renewable Utilization Probability

First, we compare the admissible ranges of wind power and the corresponding out-of-sample renewable utilization probabilities in Fig. 4. By comparing ODNE and ODNE+DRCC, we observe that their total admissible ranges are similar (see Fig. 4(c)). However, under ODNE, the allocation of the admissible ranges between W1 and W2 is unbalanced, yielding very narrow admissible ranges for W1 (see Fig. 4(a)) and very wide ones for W2 (see Fig. 4(b)). As a result, ODNE performs poorly in utilizing wind power (see Fig. 4(d)). In contrast, the allocation of admissible ranges is more balanced under ODNE+DRCC and the wind utilization becomes significantly higher and more consistent (see Fig. 4(d)) than under ODNE. This demonstrates the value of incorporating DRCC into the DNE framework. Additionally, IDNE further widens the admissible ranges and provides higher wind utilization (see Fig. 4(a)–(d)). For example, IDNE can consistently accommodates more than 95% of the wind power throughout the 24 time periods, while ODNE+DRCC accommodates less than 90% and shows a decreasing trend in renewable utilization as t increases.

TABLE I: Comparisons of Various Approaches

Approach	AvgC ($)	MaxC ($)	AvgLS (MW)	AvgWC (MW)
IDNE	56,070	102,784	0.0676	0.0901
ODNE+DRCC	56,927	127,685	0.4927	0.6904
ODNE	57,116	128,674	0.5686	1.0473
SP50	56,836	115,899	0.4649	0.1970
SP300	56,190	98,595	0.1375	0.2243

Second, we compare the actual cost in Fig. 5 and Table I. In Fig. 5, we plot the IDNE actual cost versus the ODNE

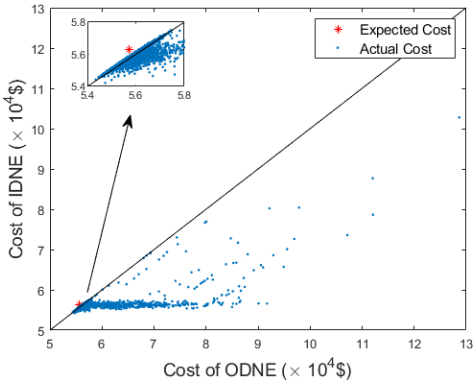

Fig. 5: Comparison on Actual Cost

actual cost for all 5,000 scenarios and the 45-degree reference line represents that the two costs agree. From this figure, we observe that most points distribute around or below the reference line, indicating that IDNE is likely to outperform ODNE in out-of-sample tests. In addition, most points line up along the horizontal line of 5.6×10^4\$, i.e., the IDNE pre-dispatch cost. This indicates that the IDNE yields stable actual costs with small variations. That is, the proposed DR approach provide stable and predictable out-of-sample performance. In Table I, we report the average actual cost (AvgC), the maximum actual cost (MaxC), the average load shedding (AvgLS), and the average wind curtailment (AvgWC) among the 5,000 scenarios. This table confirms the observations on the actual cost from Fig. 5, and further demonstrates that IDNE incurs one order of magnitude less load shedding as well as wind curtailment than ODNE does. We observe that ODNE+DRCC outperforms ODNE in almost all aspects in their out-of-sample comparisons. This confirms the value of incorporating DRCC into the DNE framework. We also test the stochastic programming model based on 50 scenarios (SP50) and 300 scenarios (SP300), respectively, and compare their out-of-sample performance with that of IDNE in Table I. From this table, we observe that IDNE outperforms both SP formulations in almost all aspects.

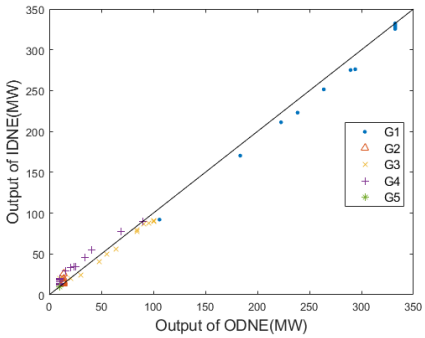

Fig. 6: Comparison on the Generation Amounts of the Thermal Units

Third, we compare the optimal pre-dispatch strategies of IDNE and ODNE in Fig. 6, from which we observe that the

pre-dispatch generation amounts of G1 and G3 under IDNE are lower than those under ODNE in most time periods. This strategy enhances the system flexibility under IDNE by preserving more ramping capability, especially when the load is high. Take the time period $t = 11$ for example, in which the load is high and G1, G3 under ODNE reach their maximum generation capacities. In this case, the upward ramping capability of ODNE becomes scarce. On the contrary, IDNE sets a lower pre-dispatch generation amounts of G1 and G3, and so preserves more (upward) ramping capability. This demonstrates how the power dispatch and DNE limits can coordinate in the proposed DRCO model to enhance the system flexibility. In addition, we observe that G1 and G3 generate 1.94% and 0.83% less power in IDNE, respectively, than they do in ODNE. This yields opportunity losses of these two generators in exchange of the higher renewable utilization. These losses can be paid off via compensation, e.g., based on the electricity price.

Finally, it takes 3.74 CPU seconds on average and 4.47 CPU seconds at maximum to solve the DRCO model with various values of δ, which verifies the tractability of the proposed approach. For comparison, the time of computing SP50 and SP300 are 6.45 seconds and 130.9 seconds, respectively.

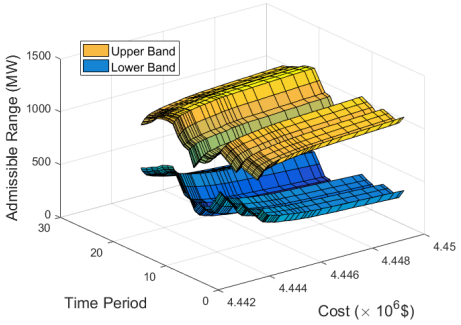

Fig. 7: Minimum Dispatch Cost vs. Admissible Ranges of Wind Power based on the Modified IEEE-118 System

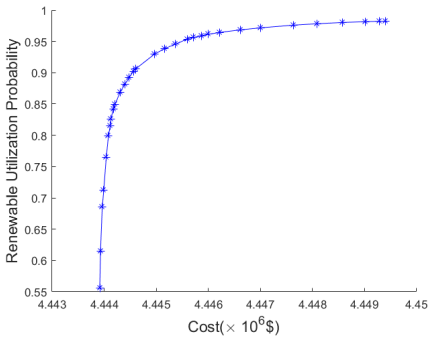

Fig. 8: The Cost-Utilization Frontier based on the Modified IEEE-118 System

D. The Modified IEEE 118-bus System and the Larger-Sized Systems

In the modified IEEE 118-bus system, there are 186 transmission lines and 54 generators providing corrective re-dispatch. Three wind farms with an identical 300 MW installed capacity are connected to the system at nodes 18, 32, and 88, respectively. The generator and network characteristics are from MATPOWER 5.1 [39] and the load profile is the same as in [19]. In addition, the wind forecasts are from the NREL Eastern Wind Dataset [40] and the mean and variance of the wind power prediction error are set as in the previous case study. The number of time periods is 24. We display the minimum power dispatch cost and the optimal DNE limits under various δ values in Fig. 7 and the cost-utilization frontier in Fig. 8. We make similar observations from these two figures on the trade-off between the power dispatch cost and the renewable utilization. Finally, it takes 18.47 CPU seconds on average and 20.25 CPU seconds at maximum to solve the DRCO model with various values of δ.

TABLE II: Computing Time for Systems of Various Sizes

System Size	14	118	300	418	600	900
CPU Seconds	3.74	18.47	61.31	118.62	223.01	537.95

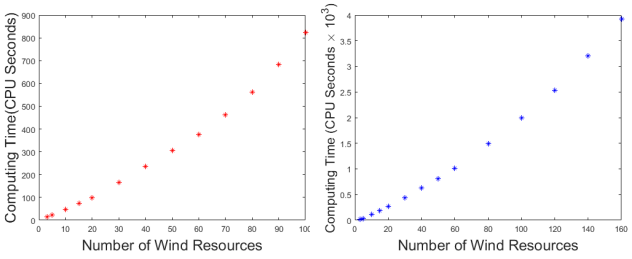

(a) (b)

Fig. 9: Computing Time for Various Numbers of Wind Resources for (a) 118-Bus System and (b) 300-Bus System

We conduct additional case studies on larger-sized systems, including the IEEE 300-bus system, 418-bus system (merged IEEE 118-bus and IEEE 300-bus systems), 600-bus system (two IEEE 300-bus systems merged), and 900-bus system (three IEEE 300-bus systems merged), all with 24 time periods. The results are summarized in Table II. From this table, we observe that our approach can be solved within 10 minutes for 118-, 300-, 418-, 600-, and 900-bus systems on a laptop, which demonstrates the scalability of the proposed method. Furthermore, we incorporate more wind resources into 118-bus and 300-bus systems, both with 24 time periods. Fig. 9(a)–(b) visualize the computing time as a function of the number of wind resources. There figures demonstrate that the proposed method is scalable in the number of uncertain parameters.

VI. Conclusion and Future Research

We propose a DRCO model for power dispatch and DNE limits. Our model incorporates an adjustable DR joint chance

constraint to explicitly measure the utilization of renewable energy. By using ADR, we derive a second order conic program that conservatively approximates the DRCO model. The case studies based on modified IEEE 14-bus and 118-bus systems demonstrate the effectiveness and computational tractability of the proposed approach. Future research includes alternative ambiguity sets and the corresponding DRCO models, as well as modeling and compensating the opportunity losses of the non-renewable resources in the IDNE approach.

Appendix A
Proof of Theorem 1

First, we observe that ambiguity set $\mathcal{D}$ satisfies Assumption (A1) in [41]. Hence, by Theorem 3 in [41], the chance constraint (4a) is equivalent to its Bonferroni approximation:

$$\inf_{\mathbb{P}_{kt}\in\mathcal{D}_{kt}} \mathbb{P}_{kt}(\varepsilon_{kt}\in[\varepsilon^{\text{L}}_{kt},\varepsilon^{\text{U}}_{kt}])\geq 1-s_{kt},\ \forall k\in[K],\ \forall t\in[T], \tag{11a}$$

$$\sum_{k\in[K]} s_{kt}\leq 1-u,\ \forall t\in[T], \tag{11b}$$

$$s_{kt}\geq 0,\ \forall k\in[K],\ \forall t\in[T], \tag{11c}$$

where $\mathbb{P}_{kt}$ represents the (marginal) probability distribution of each ε_{kt} and $\mathcal{D}_{kt}=\{\mathbb{P}_{kt}:\mathbb{E}_{\mathbb{P}_{kt}}[\varepsilon_{kt}]=\mu_{kt},\text{Var}(\varepsilon_{kt})=\sigma^2_{kt},\ \mathbb{P}_{kt}\text{ is unimodal about }\mu_{kt}\}$.

Second, chance constraint (11a) is equivalent to:

$$\inf_{\mathbb{P}_{kt}\in\mathcal{D}_{kt}} \mathbb{P}_{kt}\left(|\varepsilon_{kt}-\mu_{kt}|\leq\min\{\mu_{kt}-\varepsilon^{\text{L}}_{kt},\varepsilon^{\text{U}}_{kt}-\mu_{kt}\}\right)\geq 1-s_{kt},\ \forall k\in[K],\ \forall t\in[T], \tag{11d}$$

where $1-s_{kt}\geq u>2/3$ due to (11b). By the Gauss inequality [42], we recast (11d) as

$$1-\frac{4}{9\lambda^2_{kt}}\geq 1-s_{kt},\ \forall k\in[K],\ \forall t\in[T], \tag{11e}$$

where $\lambda_{kt}:=\min\{\mu_{kt}-\varepsilon^{\text{L}}_{kt},\varepsilon^{\text{U}}_{kt}-\mu_{kt}\}/\sigma_{kt}$.

Third, we recast inequality (11e) as second-order conic constraints (8a)–(8d) by introducing auxiliary variables r_{kt} and z_{kt} (see [43]).

Appendix B
Proof of Theorem 2

First, for given $\tau\in\mathbb{R}_+$, we compute the worst-case expectation $J(\tau):=\sup_{\mathbb{P}\in\mathcal{D}_0}\mathbb{E}_{\mathbb{P}}[\varepsilon-\tau]^+$ with $\mathcal{D}_0=\{\mathbb{P}:\mathbb{E}_{\mathbb{P}}[\varepsilon]=0,\text{Var}(\varepsilon)=1/3,\varepsilon\text{ is unimodal about }0\}$. To this end, by the unimodality of ε, there exists a random variable $\zeta\in\mathbb{R}$ such that $\varepsilon=U\zeta$, where U is uniform on $(0,1)$ and independent of ζ (see [44]). It follows that $\mathbb{E}_{\mathbb{P}}[\zeta]=0$, $\text{Var}(\zeta)=1$, and $\mathbb{E}_{\mathbb{P}}[\varepsilon-\tau]^+=\mathbb{E}_{\mathbb{P}}[h(\zeta)]$, where

$$h(\zeta)=\begin{cases}0 & \text{if }\zeta\leq 0,\\ \left[1-\frac{\tau}{\zeta}\right]^+ & \text{if }\zeta>0.\end{cases}$$

We compute $\sup_{\mathbb{P}\in\mathcal{D}_0}\mathbb{E}_{\mathbb{P}}[h(\zeta)]$ by formulating the following optimization problem:

$$\max_{\mathbb{P}}\ \int_{\mathbb{R}} h(\zeta)d\mathbb{P} \tag{12a}$$

$$\text{s.t.}\ \int_{\mathbb{R}}\zeta^2 d\mathbb{P}=1, \tag{12b}$$

$$\int_{\mathbb{R}}\zeta d\mathbb{P}=0, \tag{12c}$$

$$\int_{\mathbb{R}} d\mathbb{P}=1, \tag{12d}$$

whose dual formulation is

$$\min_{\pi}\ \pi_3+\pi_1+1 \tag{12e}$$

$$\text{s.t. }\pi_3\zeta^2+\pi_2\zeta+\pi_1+1\geq 0,\ \forall\zeta\geq 0, \tag{12f}$$

$$\pi_3\zeta^2+\pi_2\zeta+\pi_1+1\geq 1-\frac{\tau}{\zeta},\ \forall\zeta\geq 0, \tag{12g}$$

where dual variables π_3, π_2, and π_1+1 are associated with primal constraints (12b)–(12d), respectively. Dual constraint (12f) is equivalent to $\pi_1+1-(\pi_2)^2/(4\pi_3)\geq 0$, which is further equivalent to

$$\left\|\begin{bmatrix}\pi_2\\ \pi_1-\pi_3+1\end{bmatrix}\right\|_2\leq\pi_1+\pi_3+1. \tag{12h}$$

In addition, dual constraint (12g) is equivalent to $\pi_3\zeta^3+\pi_2\zeta^2+\pi_1\zeta+\tau\geq 0$ for all $\zeta\geq 0$, which is further equivalent to

$$\exists\Lambda\in\mathbb{S}^{4\times 4}_+\text{ such that:}$$

$$\Lambda_{00}=\tau, \tag{12i}$$

$$\sum_{i,j:\ i+j=2\ell-1}\Lambda_{ij}=0,\ \forall\ell=1,2,3, \tag{12j}$$

$$\sum_{i,j:\ i+j=2\ell}\Lambda_{ij}=\pi_\ell,\ \forall\ell=1,2,3 \tag{12k}$$

by Proposition 3.1(b) in [45]. It follows that $J(\tau)\equiv\sup_{\mathbb{P}\in\mathcal{D}_0}\mathbb{E}_{\mathbb{P}}[h(\zeta)]$ equals the optimal value of the following conic program:

$$\min_{\pi,\Lambda}\ \pi_3+\pi_1+1 \tag{12l}$$

$$\text{s.t. (12h)–(12k)},\ \Lambda\in\mathbb{S}^{4\times 4}_+. \tag{12m}$$

Second, we have $P^-(\varepsilon^{\text{L}},\varepsilon^{\text{U}})=\sum_{k\in[K]}\sum_{t\in[T]}c^-_{kt}\sup_{\mathbb{P}\in\mathcal{D}}\mathbb{E}_{\mathbb{P}}[\epsilon_{kt}-\epsilon^{\text{U}}_{kt}]^+$ because $\mathcal{D}$ is separable over indices k and t. But

$$\begin{aligned}&\sup_{\mathbb{P}\in\mathcal{D}}\mathbb{E}_{\mathbb{P}}\left[\epsilon_{kt}-\epsilon^{\text{U}}_{kt}\right]^+\\ &=\sqrt{3}\sigma_{kt}\sup_{\mathbb{P}\in\mathcal{D}}\mathbb{E}_{\mathbb{P}}\left[\left(\frac{\epsilon_{kt}-\mu_{kt}}{\sqrt{3}\sigma_{kt}}\right)-\left(\frac{\epsilon^{\text{U}}_{kt}-\mu_{kt}}{\sqrt{3}\sigma_{kt}}\right)\right]^+\\ &=\sqrt{3}\sigma_{kt}\ J\left(\frac{\epsilon^{\text{U}}_{kt}-\mu_{kt}}{\sqrt{3}\sigma_{kt}}\right)\end{aligned}$$

because random variable $(\epsilon_{kt}-\mu_{kt})/(\sqrt{3}\sigma_{kt})$ has mean 0, variance $1/3$, and is unimodal about 0. Hence,

$$\begin{aligned}P^-(\varepsilon^{\text{L}},\varepsilon^{\text{U}})=&\sqrt{3}\sum_{k\in[K]}\sum_{t\in[T]}c^-_{kt}\sigma_{kt}J\left(\frac{\epsilon^{\text{U}}_{kt}-\mu_{kt}}{\sqrt{3}\sigma_{kt}}\right)\\ =&g\left(\left\{\left(c^-_{kt},\frac{\varepsilon^{\text{U}}_{kt}-\mu_{kt}}{\sqrt{3}\sigma_{kt}}\right)\right\}_{k\in[K],t\in[T]}\right).\end{aligned}$$

Similarly, $P^+(\varepsilon^{\text{L}},\varepsilon^{\text{U}})=g\Big(\left\{\left(c^+_{kt},(\mu_{kt}-\varepsilon^{\text{L}}_{kt})/(\sqrt{3}\sigma_{kt})\right)\right\}_{k\in[K],\ t\in[T]}\Big)$.

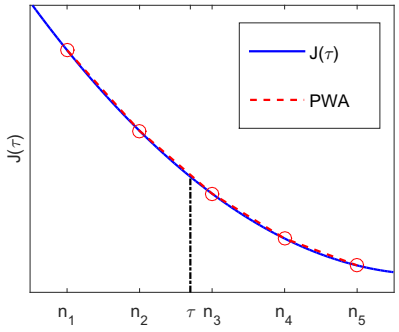

Fig. 10: An Illustration of $J(\tau)$ and its CPLA ($H = 4$)

Third, $J(\tau)$ is convex in τ because τ appears in the right-hand side of the formulation (12l)–(12m) with a minimization objective function that defines $J(\tau)$. It follows that $J(\tau)$ admits a conservative piecewise linear approximation (CPLA, see Fig. 10). Specifically, suppose that $J(\tau)$ is defined on the interval $[\tau_{\text{L}}, \tau_{\text{U}}]$. Then, letting $n_h = \tau_{\text{L}} + (h-1)(\tau_{\text{U}} - \tau_{\text{L}})/H$ for $H \in \mathbb{N}_+$ and $h \in [H+1]$, we have $J(\tau) \leq \sum_{h=1}^{H+1} \lambda_h J(n_h)$, where

$$\sum_{h=1}^{H+1} \lambda_h n_h = \tau,$$
$$\sum_{h=1}^{H+1} \lambda_h = 1, \quad \lambda_h \geq 0, \ \forall h \in [H+1].$$

Hence, $J(\tau)$ can be conservatively approximated by $\sum_{h=1}^{H+1} \lambda_h J(n_h)$. Additionally, by construction, it is clear that $\lim_{H\to\infty} \sum_{h=1}^{H+1} \lambda_h J(n_h) = J(\tau)$. For all $k \in [K]$ and $t \in [T]$, we have $0 \leq \varepsilon^{\text{U}}_{kt} \leq w^{\max}_{kt} - \hat{w}_{kt}$ and $w^{\min}_{kt} - \hat{w}_{kt} \leq \varepsilon^{\text{L}}_{kt} \leq 0$ by constraint (3). It follows that $P^-(\varepsilon^{\text{L}}, \varepsilon^{\text{U}})$ can be conservatively approximated by $\sqrt{3} \sum_{k\in[K]} \sum_{t\in[T]} \sum_{h=1}^{H+1} c^-_{kt} \sigma_{kt} \lambda^-_{hkt} J(n^-_{hkt})$, where $n^-_{1kt} = -\mu_{kt}/(\sqrt{3}\sigma_{kt})$, $n^-_{(H+1)kt} = (w^{\max}_{kt} - \hat{w}_{kt} - \mu_{kt})/(\sqrt{3}\sigma_{kt})$, $n^-_{hkt} = n^-_{1kt} + (h-1)(n^-_{(H+1)kt} - n^-_{1kt})/H$ for all $h \in [H+1]$, and

$$\sum_{h=1}^{H+1} \lambda^-_{hkt} n^-_{hkt} = \frac{\varepsilon^{\text{U}}_{kt} - \mu_{kt}}{\sqrt{3}\sigma_{kt}},$$
$$\sum_{h=1}^{H+1} \lambda^-_{hkt} = 1, \quad \lambda^-_{hkt} \geq 0, \ \forall h \in [H+1].$$

Similarly, $P^+(\varepsilon^{\text{L}}, \varepsilon^{\text{U}})$ can be conservatively approximated by $\sqrt{3} \sum_{k\in[K]} \sum_{t\in[T]} \sum_{h=1}^{H+1} c^+_{kt} \sigma_{kt} \lambda^+_{hkt} J(n^+_{hkt})$, where $n^+_{1kt} = \mu_{kt}/(\sqrt{3}\sigma_{kt})$, $n^+_{(H+1)kt} = (\mu_{kt} + \hat{w}_{kt} - w^{\min}_{kt})/(\sqrt{3}\sigma_{kt})$, $n^+_{hkt} = n^+_{1kt} + (h-1)(n^+_{(H+1)kt} - n^+_{1kt})/H$ for all $h \in [H+1]$, and

$$\sum_{h=1}^{H+1} \lambda^+_{hkt} n^+_{hkt} = \frac{\mu_{kt} - \varepsilon^{\text{L}}_{kt}}{\sqrt{3}\sigma_{kt}},$$
$$\sum_{h=1}^{H+1} \lambda^+_{hkt} = 1, \quad \lambda^+_{hkt} \geq 0, \ \forall h \in [H+1].$$

Finally, we note that the values of $J(n^{\pm}_{hkt})$ can be efficiently obtained by solving the conic program (12l)–(12m) by setting $\tau := n^{\pm}_{hkt}$. Hence, we can incorporate the conservative approximations of $P^{\pm}(\varepsilon^{\text{L}}, \varepsilon^{\text{U}})$ into the DRCO model by using a set of linear constraints.

REFERENCES

[1] L. Wu, M. Shahidehpour, and T. Li, "Stochastic security-constrained unit commitment," *IEEE Transactions on Power Systems*, vol. 22, no. 2, pp. 800–811, 2007.

[2] A. Papavasiliou, S. S. Oren, and R. P. O'Neill, "Reserve requirements for wind power integration: A scenario-based stochastic programming framework," *IEEE Transactions on Power Systems*, vol. 26, no. 4, pp. 2197–2206, 2011.

[3] Q. Wang, Y. Guan, and J. Wang, "A chance-constrained two-stage stochastic program for unit commitment with uncertain wind power output," *IEEE Transactions on Power Systems*, vol. 27, no. 1, pp. 206–215, 2012.

[4] R. Jiang, J. Wang, and Y. Guan, "Robust unit commitment with wind power and pumped storage hydro," *IEEE Transactions on Power Systems*, vol. 27, no. 2, pp. 800–810, 2012.

[5] D. Bertsimas, E. Litvinov, X. A. Sun, J. Zhao, and T. Zheng, "Adaptive robust optimization for the security constrained unit commitment problem," *IEEE Transactions on Power Systems*, vol. 28, no. 1, pp. 52–63, 2013.

[6] J. Zhao, T. Zheng, and E. Litvinov, "Variable resource dispatch through do-not-exceed limit," *IEEE Transactions on Power Systems*, vol. 30, no. 2, pp. 820–828, 2015.

[7] W. Wei, F. Liu, and S. Mei, "Dispatchable region of the variable wind generation," *IEEE Transactions on Power Systems*, vol. 30, no. 5, pp. 2755–2765, 2015.

[8] C. Shao, X. Wang, M. Shahidehpour, X. Wang, and B. Wang, "Security-constrained unit commitment with flexible uncertainty set for variable wind power," *IEEE Transactions on Sustainable Energy*, vol. 8, no. 3, pp. 1237–1246, 2017.

[9] S. Zymler, D. Kuhn, and B. Rustem, "Distributionally robust joint chance constraints with second-order moment information," *Mathematical Programming*, vol. 137, no. 1-2, pp. 167–198, 2013.

[10] W. Wiesemann, D. Kuhn, and M. Sim, "Distributionally robust convex optimization," *Operations Research*, vol. 62, no. 6, pp. 1358–1376, 2014.

[11] R. Jiang and Y. Guan, "Data-driven chance constrained stochastic program," *Mathematical Programming*, vol. 158, no. 1-2, pp. 291–327, 2016.

[12] J. Zhao, T. Zheng, and E. Litvinov, "A unified framework for defining and measuring flexibility in power system," *IEEE Transactions on Power Systems*, vol. 31, no. 1, pp. 339–347, 2016.

[13] W. Wei, F. Liu, and S. Mei, "Real-time dispatchability of bulk power systems with volatile renewable generations," *IEEE Transactions on Sustainable Energy*, vol. 6, no. 3, pp. 738–747, 2015.

[14] Z. Li, W. Wu, B. Zhang, and B. Wang, "Robust look-ahead power dispatch with adjustable conservativeness accommodating significant wind power integration," *IEEE Transactions on Sustainable Energy*, vol. 6, no. 3, pp. 781–790, 2015.

[15] ——, "Adjustable robust real-time power dispatch with large-scale wind power integration," *IEEE Transactions on Sustainable Energy*, vol. 6, no. 2, pp. 357–368, 2015.

[16] W. Wei, J. Wang, and S. Mei, "Dispatchability maximization for co-optimized energy and reserve dispatch with explicit reliability guarantee," *IEEE Transactions on Power Systems*, vol. 31, no. 4, pp. 3276–3288, 2016.

[17] C. Shao, X. Wang, M. Shahidehpour, X. Wang, and B. Wang, "Power system economic dispatch considering steady-state secure region for wind power," *IEEE Transactions on Sustainable Energy*, vol. 8, no. 1, pp. 268–278, 2017.

[18] B. Zeng and L. Zhao, "Solving two-stage robust optimization problems using a column-and-constraint generation method," *Operations Research Letters*, vol. 41, no. 5, pp. 457–461, 2013.

[19] C. Wang, F. Liu, J. Wang, F. Qiu, W. Wei, S. Mei, and S. Lei, "Robust risk-constrained unit commitment with large-scale wind generation: An adjustable uncertainty set approach," *IEEE Transactions on Power Systems*, vol. 32, no. 1, pp. 723–733, 2017.

[20] C. Wang, F. Liu, J. Wang, W. Wei, and S. Mei, "Risk-based admissibility assessment of wind generation integrated into a bulk power system," *IEEE Transactions on Sustainable Energy*, vol. 7, no. 1, pp. 325–336, 2016.

[21] F. Qiu, Z. Li, and J. Wang, "A data-driven approach to improve wind dispatchability," *IEEE Transactions on Power Systems*, vol. 32, no. 1, pp. 421–429, 2017.

[22] Z. Li, F. Qiu, and J. Wang, "Multi-period do-not-exceed limit for variable renewable generation dispatch considering discrete recourse controls," *arXiv preprint arXiv:1608.05273*, 2016.

[23] A. S. Korad and K. W. Hedman, "Zonal do-not-exceed limits with robust corrective topology control," *Electric Power Systems Research*, vol. 129, pp. 235–242, 2015.

[24] A. S. Korad and K. W. Hedman, "Enhancement of do-not-exceed limits with robust corrective topology control," *IEEE Transactions on Power Systems*, vol. 31, no. 3, pp. 1889–1899, 2016.

[25] P. Xiong, P. Jirutitijaroen, and C. Singh, "A distributionally robust optimization model for unit commitment considering uncertain wind power generation," *IEEE Transactions on Power Systems*, vol. 32, no. 1, pp. 39–49, 2017.

[26] Y. Zhang, S. Shen, and J. L. Mathieu, "Distributionally robust chance-constrained optimal power flow with uncertain renewables and uncertain reserves provided by loads," *IEEE Transactions on Power Systems*, vol. 32, no. 2, pp. 1378–1388, 2017.

[27] W. Xie and S. Ahmed, "Distributionally robust chance constrained optimal power flow with renewables: A conic reformulation," *IEEE Transactions on Power Systems*, vol. 33, no. 2, pp. 1860–1867, 2018.

[28] C. Zhao and R. Jiang, "Distributionally robust contingency-constrained unit commitment," *IEEE Transactions on Power Systems*, vol. 33, no. 1, pp. 94–102, 2018.

[29] P. M. Esfahani and D. Kuhn, "Data-driven distributionally robust optimization using the wasserstein metric: Performance guarantees and tractable reformulations," *Mathematical Programming*, Forthcoming, 2017.

[30] C. Wang, R. Gao, F. Qiu, J. Wang, and L. Xin, "Risk-based distributionally robust optimal power flow with dynamic line rating," *arXiv preprint arXiv:1712.08015*, 2017.

[31] Y. Chen, Q. Guo, H. Sun, Z. Li, W. Wu, and Z. Li, "A distributionally robust optimization model for unit commitment based on kullback-leibler divergence," *IEEE Transactions on Power Systems*, Forthcoming, 2018.

[32] B. Li, R. Jiang, and J. L. Mathieu, "Distributionally robust risk-constrained optimal power flow using moment and unimodality information," in *Decision and Control (CDC), 2016 IEEE 55th Conference on*. IEEE, 2016, pp. 2425–2430.

[33] ——, "Ambiguous risk constraints with moment and unimodality information," *Mathematical Programming*, pp. 1–42, 2017.

[34] S. Fink, C. Mudd, K. Porter, and B. Morgenstern, "Wind energy curtailment case studies," National Renewable Energy Laboratory Report, Tech. Rep., 2009, available at http://www.nrel.gov/docs/fy10osti/46716.pdf.

[35] R. Doherty and M. O'malley, "A new approach to quantify reserve demand in systems with significant installed wind capacity," *IEEE Transactions on Power Systems*, vol. 20, no. 2, pp. 587–595, 2005.

[36] J. Wang, M. Shahidehpour, and Z. Li, "Security-constrained unit commitment with volatile wind power generation," *IEEE Transactions on Power Systems*, vol. 23, no. 3, pp. 1319–1327, 2008.

[37] B.-M. Hodge, D. Lew, M. Milligan, H. Holttinen, S. Sillanpää, E. Gómez-Lázaro, R. Scharff, L. Söder, X. G. Larsén, G. Giebel, D. Flynn, and J. Dobschinski, "Wind power forecasting error distributions: An international comparison," in *11th Annual International Workshop on Large-Scale Integration of Wind Power into Power Systems as well as on Transmission Networks for Offshore Wind Power Plants Conference*, 2012.

[38] A. L. Soyster, "Convex programming with set-inclusive constraints and applications to inexact linear programming," *Operations Research*, vol. 21, no. 5, pp. 1154–1157, 1973.

[39] R. D. Zimmerman, C. E. Murillo-Sánchez, and R. J. Thomas, "Matpower: Steady-state operations, planning, and analysis tools for power systems research and education," *IEEE Transactions on power systems*, vol. 26, no. 1, pp. 12–19, 2011.

[40] "NREL Eastern Wind Dataset," https://www.nrel.gov/grid/eastern-wind-data.html, accessed: 2018-07-30.

[41] W. Xie, S. Ahmed, and R. Jiang, "Optimized bonferroni approximations of distributionally robust joint chance constraints," *Available at Optimization Online*, 2017.

[42] C.-F. Gauss, *Theoria combinationis observationum erroribus minimis obnoxiae*. Henricus Dieterich, 1823, vol. 1.

[43] A. Ben-Tal and A. Nemirovski, *Lectures on modern convex optimization: analysis, algorithms, and engineering applications*. SIAM, 2001, vol. 2.

[44] S. Dharmadhikari and K. Joag-Dev, *Unimodality, Convexity, and Applications*. Elsevier, 1988.

[45] D. Bertsimas and I. Popescu, "Optimal inequalities in probability theory: A convex optimization approach," *SIAM Journal on Optimization*, vol. 15, no. 3, pp. 780–804, 2005.

[46] B. Tsuchiya, "A convergence analysis of the scaling-invariant primal-dual path-following algorithms for second-order cone programming," *Optimization Methods and Software*, vol. 11, no. 1-4, pp. 141–182, 1999.

Hongyan Ma received her B.S. degree in Electrical Engineering from Shandong University, Jinan, China, in 2013. She is currently pursuing the Ph.D. degree in Electrical Engineering at Shanghai Jiao Tong University, Shanghai, China. She was also a visiting scholar at the University of Michigan, Ann Arbor, MI, USA. Her research interests include power system operation, optimization, and renewable energy integration.

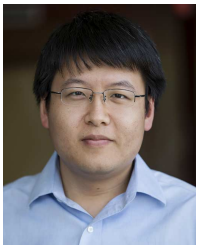

Ruiwei Jiang (M'14) received the B.S. degree in Industrial Engineering from the Tsinghua University, Beijing, China, in 2009, and the Ph.D. degree in Industrial and Systems Engineering from the University of Florida, Gainesville, FL, USA, in 2013. He is currently an Assistant Professor with the Department of Industrial and Operations Engineering, University of Michigan, Ann Arbor, MI, USA. His research interests include power system planning and operations, renewable energy management, and water distribution operations and system analysis.

Zheng Yan received the B.S. degree in Electrical Engineering from Shanghai Jiao Tong University, Shanghai, China, in 1984 and the M.S. and Ph.D. degrees in Electrical Engineering from Tsinghua University, Beijing, China, in 1987 and 1991, respectively. He is currently a Professor in the Department of Electrical Engineering at Shanghai Jiao Tong University, Shanghai, China. His research interests are in application of optimization theory to power systems, power markets and dynamics security assessment.